Experimental results on a chiller using a CO2-DME mixture

G. Vaccaro, A. Milazzo, Pascal Tobaly, Ahmadou Tidiane Diaby, L. Talluri

International Journal of Refrigeration 168 (2024) 662–672

Contents lists available at ScienceDirect

International Journal of Refrigeration

journal homepage: www.elsevier.com/locate/ijrefrig

INSTITUT INTERNATIONAL DU FROID
INTERNATIONAL INSTITUTE OF REFRIGERATION

Experimental results on a chiller using a CO_2-DME mixture

Résultats expérimentaux sur un refroidisseur utilisant un mélange CO2-DME

G. Vaccaro [a,*], A. Milazzo [a], P. Tobaly [b], A.T. Diaby [b], L. Talluri [a]

[a] *Department of Industrial Engineering, University of Florence, Florence, Via S. Marta 3, 50139, Italy*
[b] *Laboratoire du froid et système énergétiques et thermiques (Lafset), Cnam, 292 rue Saint Martin 75003, France*

A R T I C L E I N F O

Keywords:
Chiller
Co2
Dme
Mixtures
Refrigeration cycle
Thermodynamics
Mots clés:
Refroidisseur
Co2
Dme
Mélanges
Cycle frigorifique
Thermodynamique

A B S T R A C T

CO_2-DME (Carbon Dioxide-Dimethyl Ether) mixtures raised our interest in the last year as they promise to increase the COP with respect to pure CO_2 while maintaining GWP = 1. The mixture can be non-flammable, as far as the percentage of DME is low. This study presents experimental findings obtained from a chiller system utilizing CO_2-DME mixtures as the working fluid. The experimental investigation aims to analyse the performance and behaviour of the chiller under varying operating conditions. Key parameters, such as coefficient of performance, cooling capacity, and thermodynamic behaviour are examined to assess the suitability and efficacy of the CO_2-DME mixture in chiller applications. The experimental results shed light on the thermodynamic characteristics and operational considerations of the chiller system, providing valuable insights into the potential of CO_2-DME mixtures for environmentally friendly, safe and energy-efficient cooling technologies. The experimental findings indicate a maximum increase in COP of 15 % for a mixture comprising 10 % DME, with a condensation temperature of 35 °C. Furthermore, the cooling capacity is reduced only by 7 % in the worst case.

1. Introduction

The literature on CO_2–based mixtures as working fluids in refrigeration systems is rapidly increasing. These mixtures may combine the high volumetric cooling capacity and low GWP of CO_2 with a reduced pressure at the gas cooler (or condenser, if the mixture allows a subcritical working cycle) and a temperature glide at the evaporator, which may be beneficial in order to improve the heat exchange with the cold fluid delivered to the user. This concept has been discussed since the first decade of this century. Experimental results on CO_2 and propane mixtures have been published for example by Tobaly et al. (2018).

A very recent experimental work on a mixture of CO_2 and R152a has been presented by Sicco et al. (2024), showing that a maximum COP improvement of 11.6 % can be achieved with a mixture featuring a 5 % of R152a. Mixtures with R152a have been used also by Martínez-Ángeles et al. (2024).

Yu et al. (2018) investigated CO_2/propane mixtures for automobile air conditioning. They obtained a COP increase up to 29.4 % with fixed compressor speed and of 22 % with fixed cooling capacity. The same authors (Yu et al., 2019) also investigated CO_2/R41 mixtures obtaining a COP increase of 14.5 % and 25.7 % respectively for heating and cooling mode.

Sanchez et al. (2023) investigated a CO_2 vertical beverage cooler using binary mixtures of CO_2/R1270 (92.5/7.5 %) and CO_2/R32 (78/22 %) in a configuration with an IHX. Their findings indicated energy savings of up to 15.7 % and 17.2 % respectively, under class III climate conditions (25 °C, 60 %).

Sanchez et al. (2024) examined a refrigeration plant in two configurations, with and without an IHX, using three different mixtures. They found that the mixture with R32 performed best in both configurations, achieving COP increases of 15.3 % and 22.2 %.

The works on CO_2-DME mixtures are less numerous. Onaka et al. (2008) did a thermodynamic analysis of a heat pump cycle using CO_2/DME mixture, and found 10 % mass DME as the local optimal composition for their boundary conditions.

Koyama et al. (2007) did an experimental analysis with 10 % DME, both in cooling and heating mode, for a cycle without IHX. They found almost the same maximum COP for pure CO_2 and mixture. When using the mixture, the optimal discharge pressure is reduced by 2 and 1.9 MPa

* Corresponding author.
E-mail address: guglielmo.vaccaro@unifi.it (G. Vaccaro).

https://doi.org/10.1016/j.ijrefrig.2024.10.002
Received 15 March 2024; Received in revised form 27 August 2024; Accepted 3 October 2024
Available online 5 October 2024

Nomenclature

c_p	Specific heat capacity (kJ/kgK)
h	Enthalpy (kJ/kg)
$\dot{m}$	Mass flow rate (kg/h)
P	Pressure (bar)
Q_{ref}	Cooling capacity (W)
ρ	Density (kg/m^3)
T	Temperature (K)
$\dot{V}$	Volumetric flow rate (l/min)
W	Work (W)
x	Mass concentration (kg kg^{-1})
COP	Coefficient of performance [-]
DME	Dimethyl ether
EVA	Evaporator
GC	Gas Cooler
HP	High Pressure
IHX	Internal Heat Exchanger

subscripts

f	refrigerant fluid
in	inlet
liq	Liquid
vap	Vapour
w	Water
wg	Water-glycol

and the discharge temperature is increased by 16 and 13 K for heating and cooling mode respectively.

Di Nicola et al. (2011) did an analysis for a cascade refrigeration system with the low temperature cycle employing different mixtures of natural refrigerants. They found that the addition of small quantities of CO_2 brings a little reduction of COP, but also a reduction of GWP and flammability, maintaining the possibility to evaporate below the CO_2 triple point.

Starting from the same idea, Massuchetto et al. (2019) did an analysis for a cascade system and decided to use a mixture of CO_2/ammonia for the high temperature cycle, in order to decrease the heat exchanger losses. For the low temperature cycle, they found that the best mixture was CO_2/DME (10 % CO_2), which brought an efficiency increase up to 30 %

Onaka et al. (2010) also did an experimental study on evaporation heat transfer of a CO_2/DME mixture in a horizontal smooth tube. Starting from pure DME they obtained a reduction of HTC of 20 % for 10 % CO_2 and of 48 % for 25 % CO_2

Afroz et al. (2008) did an experimental study on heat transfer and pressure drop during in-tube condensation for 21 % and 39 % mass of CO_2, finding a decrease of HTC and pressure drop when increasing CO_2.

A recent review of several mixtures working on various cycle configurations has been presented by Vaccaro et al. (2023). Soon after, the same authors have decided to concentrate on mixtures of CO_2 and hydrocarbons (Vaccaro et al. 2024), showing that DME (Dimethyl ether) may be the best option in terms of performance and safety.

The present work is mainly intended to verify the theoretical results presented by Vaccaro et al. (2024). To this aim, the experimental facility used by Tobaly et al. (2018) is particularly well suited. The scroll compressor is quite robust with respect to liquid ingestion, and this has allowed to explore low superheating values at compressor inlet. A favourable consequence of this choice is the reduction of the compressor exit temperature. With respect to the other experimental work on CO_2/DME mixture (Koyama et al., 2007), the introduction of a IHX has proven fundamental and has produced a significantly higher COP. Moreover, the extensive discussion about the IHX and its role in the cycle forms another important contribution of this paper. In the previous literature the IHX receives the fluid in superheated state from the evaporator, while in our experiments the temperature glide featured by zeotropic mixtures is split between the evaporator and the IHX, in order to optimize the low temperature side of the cycle as a whole.

The experimental results presented herein enlarge those described by Tobaly et al. (2018). As suggested by the calculations performed by Vaccaro et al. (2024), low quantities of DME are used as additive in the CO_2 mixture. In this way, a low-GWP, non-flammable refrigerant, featuring improved performance over pure CO_2, is obtained.

2. Experimental details

2.1. Experimental setup

The experiments have been carried on a refrigeration system comprising a scroll compressor, brazed-plate heat exchangers, an electronic expansion valve, a liquid separator and an internal heat exchanger IHX. The experimental apparatus has been first described in Bouteiller et al. (2015) and is shown in Fig. 1. The circuit is based on a 3.5 kW water-to-water heat pump. A Sanden hermetic scroll compressor with 4 cm^{3}vol is used. The compressor speed may be varied from 1200 to 5500 rpm through a continuous 0 - 5 V signal. In order to maintain homogeneity in the measurements, the entire experimental campaign presented herein was carried out at 2.5 V.

The test bench was specifically designed for tests with refrigerant mixtures. The apparatus has been used for tests in heat pump configuration till 2017 (Bouteiller et al., 2017). Later, its use has been extended to refrigeration and air conditioning (Tobaly et al., 2018). External working conditions are set by means of two auxiliary water loops. On the gas cooler side, the inlet water temperature is regulated by a thermostatic bath and the flow rate is adjusted by a valve. On the evaporator side, a 32 % water/glycol mixture is used and its inlet temperature is regulated using an electrical heater. The flow rate in this loop can be adjusted to reach the targeted outlet temperature. Flow rates in the auxiliary loops are given by electromagnetic flow meters.

The system is controlled by a high-pressure electronic valve and two manually operated valves fitted at the separator liquid and vapour exits. In this way, the maximum cycle pressure P_1 and the superheat at the compressor inlet can be controlled.

The internal heat exchanger should also act as a liquid reservoir/separator at compressor inlet. However, in some cases, the liquid level has changed significantly, either exposing the coil to dry vapour (and hence reducing the heat exchange) or overcoming the entrance of the exit pipe (and hence causing liquid ingestion by the compressor).

2.2. Measurement instrument

The circuit is fully instrumented for the complete characterization of the refrigerant state throughout the cycle. Two Coriolis flow meters (0.15 % accuracy in the range 4 - 400 kg/h) are installed after the liquid vapour separator, one on the liquid line and one on the vapour line. A wattmeter measures the electric input to the compressor. The thermodynamic conditions are measured by T-type thermocouples (copper and constantana wires, measuring range between −200 °C and 200 °C, with a maximum error of ± 0.5 K), and piezo resistive pressure transducers (Endress Hauser, 0.03 % in the range 0 - 96–78.4 bar). The thermocouples have been specifically calibrated in a narrow range (−10 °C to

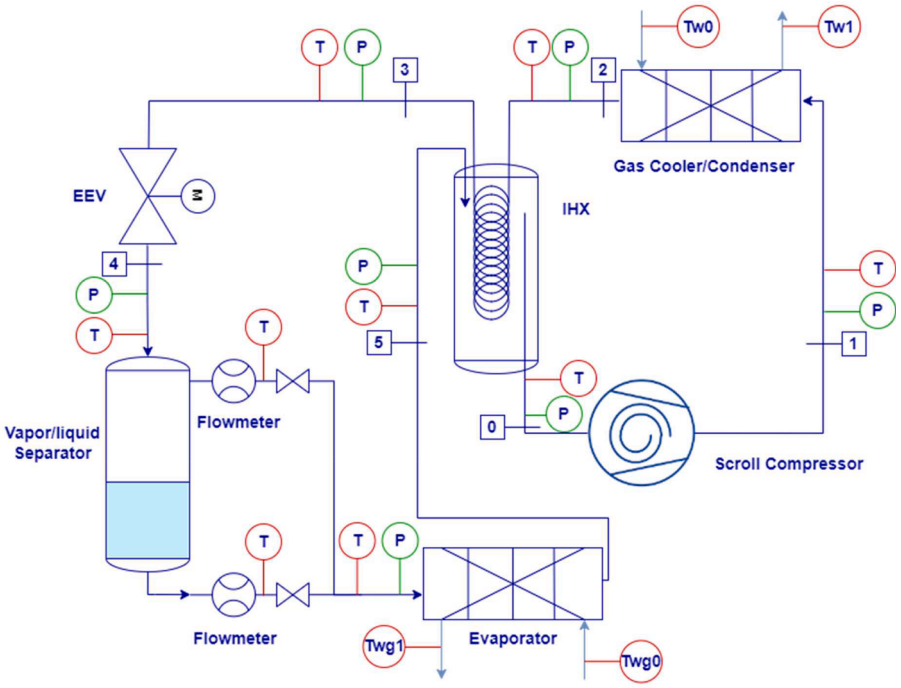

Fig. 1. Experimental setup: P pressure transducers, T thermocouples.

Table 1
Measuring instrument and accuracy.

Sensors	Type / Supplier	Accuracy
Pressure transducers	Cerabar M / Endress Hauser	0.04 % on the range 0.96 – 137.7 bar. 0.03 % on the range 0.96 – 78.4 bar.
Refrigerant mass flow meters	Promag 83 / Endress Hauser	0.15 % in the range 4 – 400 kg/h (with 3/8″ tube). 0.1 % in the range 4 – 90 kg/h (with 1/8″ tube).
Magnetic flow meters	Promag 10H08 / Endress Hauser	0.5 % on the range 0.5 – 30 l/min.
Wattmeter	μTAC300 / Sfere	0.5 % on the power range 500 – 1500 W.
Thermocouples	Class 1 T type/TC	0.05 °C on the range −10 °C – +40 °C

+40 °C), in order to increase their accuracy, with a PT100 (PT-102–14H) that has maximum error of 30.6 mK and a repeatability of 0.005 K Bouteiller (2017). The calibration has been performed according to the advice of the Joint Metrology Laboratory (LCM LNE) of the CNAM in St Denis. The PT100 is inserted in a copper cylinder to protect it from shocks and limit temperature gradients. The inside of the cylinder was flushed with nitrogen to remove humidity and filled with thermal paste (Apiezon N). A thin stainless-steel tube is brazed onto one end of the cylinder to protect the probe cables and allow handling. The metal body and probe stem are grounded. The sensibility of the data acquisition NI 9214 is 0.01 K. The resulting error of the calibrated thermocouple is:

$$e = 0.0306 + 0.005 + 0.01 = 0.0456\ K \tag{1}$$

All signals were acquired by a National Instruments compact DAQ platform 9174 (combined with NI9214 thermocouple modules, NI9203 current module for pressure transducers, NI9263 for signal output of compressor inverter) and processed by a software specifically developed in LabView environment. Table 1 summarizes the measurements ranges and accuracy of the measuring instruments.

2.3. Coefficient of performance

The COP of the refrigeration system is defined as:

$$COP = \frac{\dot{m}_{wg} c_{pwg} \Delta T_{wg}}{P_{comp}} \tag{2}$$

where $\dot{m}_{wg}$ is the water/glycol mass flow rate, c_{pwg} is its specific heat, ΔT_{wg} is its temperature difference and P_{comp} is the electrical power input of the compressor.The error on the calculated COP (see below) may therefore be estimated as follows:

$$\frac{dCOP}{COP} = \frac{dW}{W} + \frac{dc_{pwg}}{c_{pwg}} + \frac{d\rho_{wg}}{\rho_{wg}} + \frac{d\dot{V}_{wg}}{\dot{V}_{wg}} + \frac{d\Delta T_{wg}}{\Delta T_{wg}} \tag{3}$$

Given the measurement uncertainties reported in Table 1, the maximum error comes out to be 3.04 %. As a further proof of the accuracy of data, the COP for pure CO_2 has been calculated in two ways, one relying on the cooling power evaluated on the water/glycol flow and the other evaluated on the refrigerant side. The results obtained are quite close, with an average difference between the two of only 2.5 % and a maximum of 4.8 %.

3. Results

This work presents results for various compositions and water temperature at gas-cooler exit T_{w0}. All results are obtained for a water-glycol inlet and outlet temperature in the evaporator of 7 and 12 °C respectively.

The percentage of DME has been obtained by mixing with utmost care the due masses of CO_2 and DME during the filling of the circuit. The scales have an error, which may be pessimistically evaluated in 5 g for the one weighting the CO_2 and 1 g for the one weighting the DME. Therefore, considering that the total mass of refrigerant is 800 gs, when

5 % of DME is added, the real percentage may vary between 4.85 % and 5.15 %. When 10 % of DME is added, the real percentage may vary between 9.82 % and 10.18 %.

The differences found, however, are much bigger. Significant discrepancies between weighted and circulant compositions have been reported also by other authors. For example, Bouteiller (2017) has found the same problem for mixtures of CO_2 and propane. A possible reason may be the fact that the liquid mixture stored in the separators is richer in the less volatile compound (DME), leaving the vapour phase richer in CO_2. A second issue is related to the absorption of refrigerants by the lubricant oil. Caramaschi et al. (2024) have shown that DME is even more soluble in oil than propane. This issue is hence surely present also in our case. A third issue is the velocity difference between the liquid and vapor phase in heat exchangers. If liquid and vapor have different compositions, this may further enrich the mixture in the most volatile component. Experimental results on the mixture composition problems have been published also by Youby Idrissi (2003).

3.1. COP analysis

Fig. 2 shows the COP of the different compositions of mixtures studied for various experimental conditions. In all cases, the addition of DME increases the system COP. Obviously the COP increases for decreasing T_{w0}. The three curves on the lower part of the diagram, referred to $T_{w0} = 40°C$, are rather flat around the optimum and clearly show a best result for a 10 % of DME in the mixture. By the way, the optimum is reached for a significantly lower value of the maximum cycle pressure P_1 (below 85 bars), which is >10 bars lower than the optimum for pure CO_2. The three curves referred to $T_{w0} = 35°C$ are shorter, i.e. the system is more sensitive to small variations in the maximum cycle pressure. However, the convenience of the 10 % DME mixture is very evident and on average reaches a 15 % improvement over pure CO_2. The optimum value of P_1 is as low as 75 bars. A difference is evident between the results on top of the diagram and the others: these results are obtained with a subcritical cycle, being $T_{w0} = 30°C$. The trend in terms of COP is more difficult to read. Moreover, the best results in this case are obtained for a mixture with 5 % DME at maximum cycle pressure around 72 bars. In the following section, we analyze all cases in further detail. The Ph digrams shown in the following sections are all referred to the optimum condition, i.e. the one that gives the highest COP for a given set of boundary conditions, marked with a star in Fig. 2.

In order to have a further insight in these results, we have used the model presented in Vaccaro et al. (2024). A comparison has been carried on between the parameters calculated using the Refprop version 10 database (Lemmon et al. 2018) and those measured in each point. This comparison shows a significant difference between the composition of the mixture introduced in the circuit and the one that must be used within the model in order to reproduce the experimental measurements.

3.2. Thermodynamic analysis

The experimental results shown above have been used to calculate the thermodynamic cycle of the system. Points 0, 1, 2 and 3 are directly calculated from measured temperature and pressure. Point 4 is calculated from the measured pressure and from the quality, which is calculated from the mass flow rates measured by the Coriolis flow meters shown in Fig. 1. This quality has been checked imposing a constant enthalpy transformation between points 3 and 4. Fig. 3 shows that the agreement between the two methods is very good. The average absolute difference is 0.88 % with pure CO_2 (Fig. 3a). In the case of mixtures, the average absolute difference is 0.92 % (Fig. 3b).

Point 5 has been calculated by adding the heat exchanged on the water/glycol side in the evaporator to the enthalpy of point 4.

A further validation has been performed on the heat exchangers, comparing the measurements obtained on the water and water/glycol sides with those obtained on the refrigerant side. The results for pure CO_2 are shown in Fig. 4a and 4b, showing that all points are within ±5 %. The only exception is the blue point below the −5 % line, which is related to a $P_1 = 74.37$ bar. In this condition, the gas cooler exit (point 2) is located on a rather flat isotherm and hence a small error in pressure translates in a large enthalpy difference.

On the gas cooler/condenser side, the relative error averaged on all data points, in absolute value,

$$e_{gc} = \left| \frac{\dot{m}_w c_{pw} \Delta T_w - \dot{m}_f (h_1 - h_2)}{\dot{m}_w c_{pw} \Delta T_w} \right| \tag{4}$$

comes out to be 1.9 % for pure CO_2.

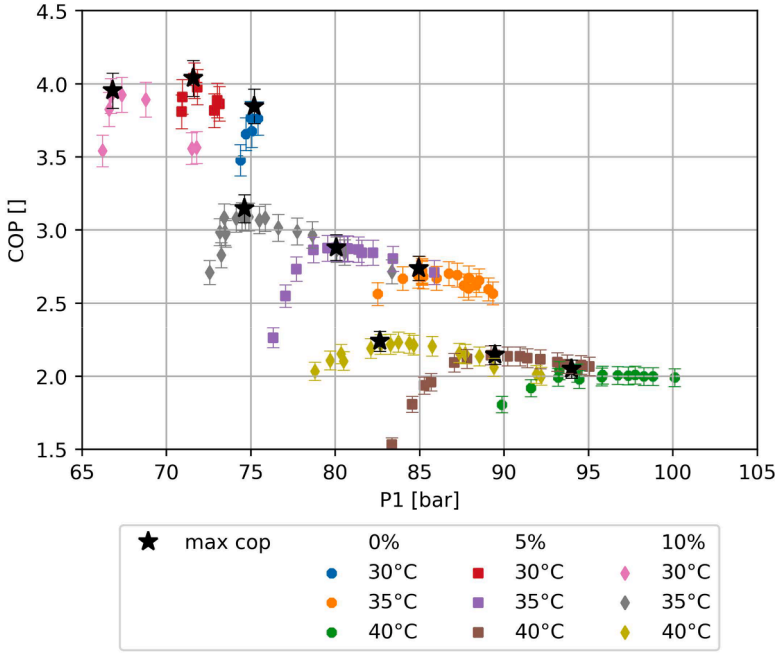

Fig. 2. Synopsis of the COP results.

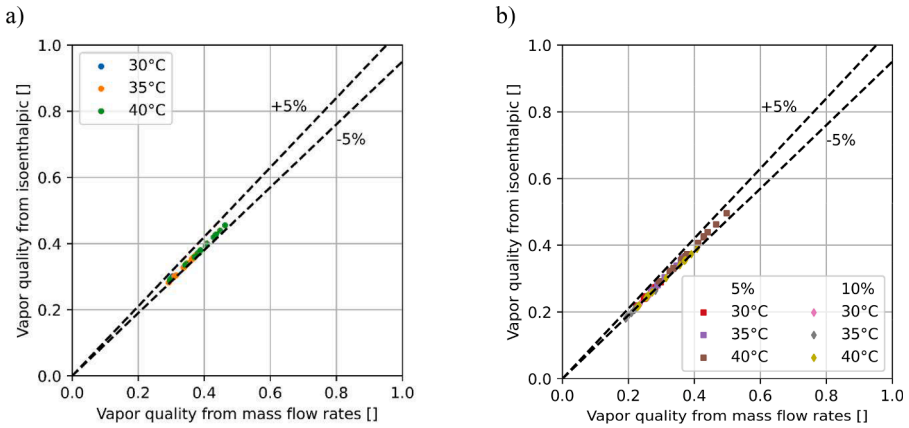

Fig. 3. Vapor quality validation: a) Pure CO_2, b) Mixtures.

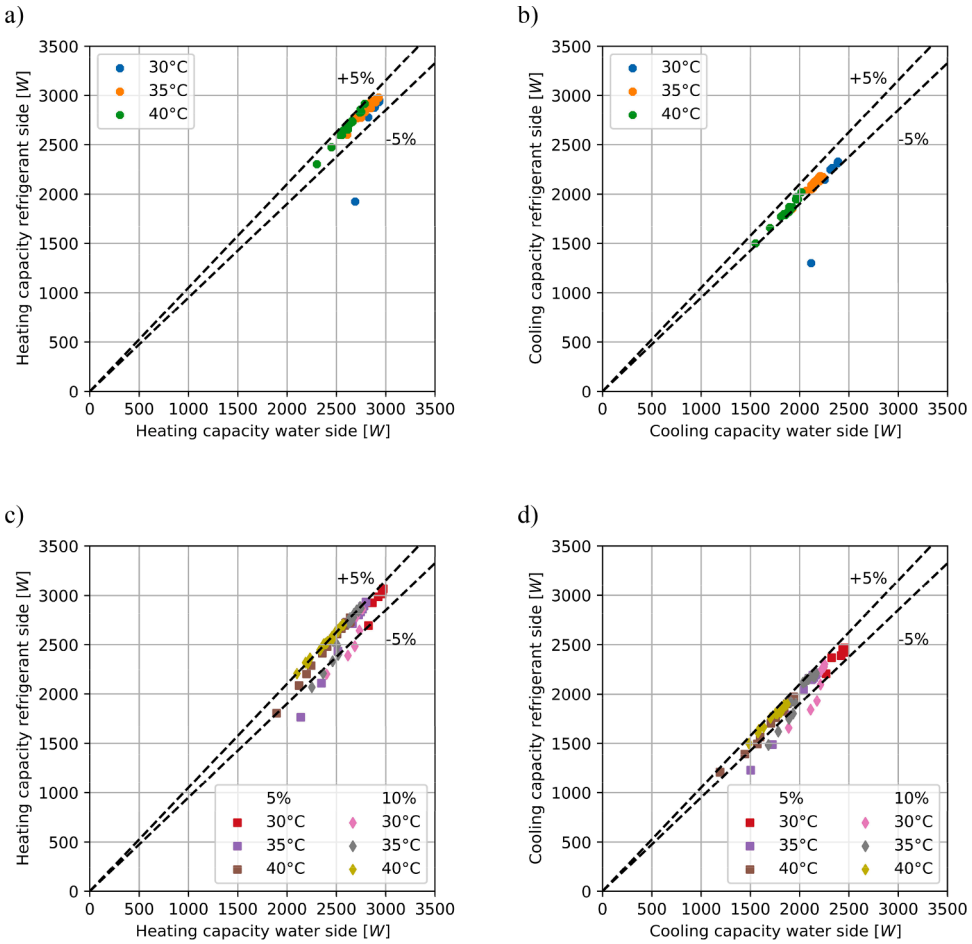

Fig. 4. Heat transfer validation: a) Heating capacity pure CO_2, b) Cooling capacity pure CO_2 c) Heating capacity mixtures, d) Cooling capacity mixtures.

For what concerns mixtures, the results are affected also by the uncertainty in composition. Anyway, results of heating capacity validation are shown in Fig. 4c, and the relative error averaged on all data points, in absolute value, is 4.4 %.

On the cold side, the heat exchanged with the water/glycol may be compared with the heat received by the working fluid, being point 5 obtained by starting from point 0 and subtracting the heat exchanged in the IHX.

$$e_{eva} = \left| \frac{\dot{m}_{wg} c_{pwg} \Delta T_{wg} - \dot{m}_f [h_0 - (h_2 - h_3) - h_4]}{\dot{m}_w c_{pw} \Delta T_{wg}} \right| \quad (5)$$

The average relative error in absolute value is 2.5 % for pure CO_2 (Fig. 4b) and 3.0 % for mixtures (Fig. 4d).

For what concerns the mixture composition, we have used the iterative method proposed by Johansson et al. (2001) that postulates an isoenthalpic expansion and modifies the circulating composition until convergence.

Fig. 5 shows that tests performed with a measured DME percentage of 5 % and 10 % actually have a circulating composition around 2 % and 5 % respectively. Obviously, these are not the precise compositions of the mixture circulating within the system, but undoubtely show that the

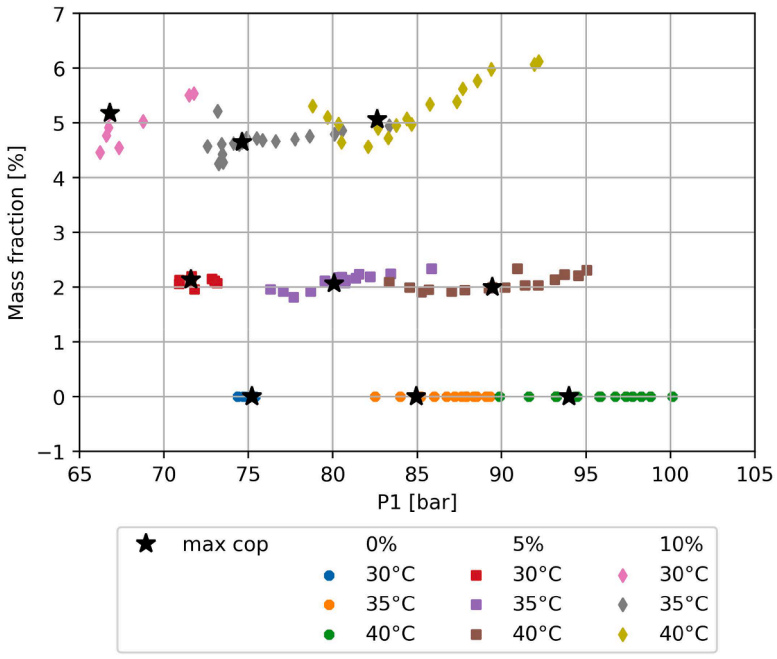

Fig. 5. Calculated circulating composition.

DME percentage during the system operation is significantly lower than expected. Once more, it is proven that DME is able to change significantly the properties of CO_2, even when added in very small quantities.

When dealing with mixtures, REFPROP introduces an additional source of error by overestimating the critical pressure of the mixture (note that the term "pseudo-critical pressure" should be used for mixtures, but the shorter version has been used here for the sake of simplicity). The results calculated by REFPROP may be compared to the experimental results for CO_2 and DME obtained by Tsang and Streett (1981), showing evident discrepancies. Luckily, the temperatures and DME concentrations used in our experiments are moderate, and hence the error is acceptable. Furthermore, as shown by Caramaschi et al. (2022), REFPROP is more robust than other options when modeling mixtures of CO_2 and other fluids.

3.2.1. *Case* $T_{w0} = 30\ ^{\circ}C$

As a reference, let's first consider the Ph diagram of the cycle operating with pure CO_2 (Fig. 6a). The maximum cycle pressure is practicly equal to the CO_2 critical pressure.

In this case, there is obviously no glide on the lower side of the cycle. The condenser pressure is 75 bar. The electric power absorbed by the compressor is 620 W, while the cooling power is 2390 W, giving a COP of 3.85. This result is obtained when the fluid condition at evaporator exit is saturated vapour. The superheating at compressor inlet, i.e. 4.3 °C, is completely given by the IHX.

The IHX heat transfer capacity is weak, as can be seen by the short Δh

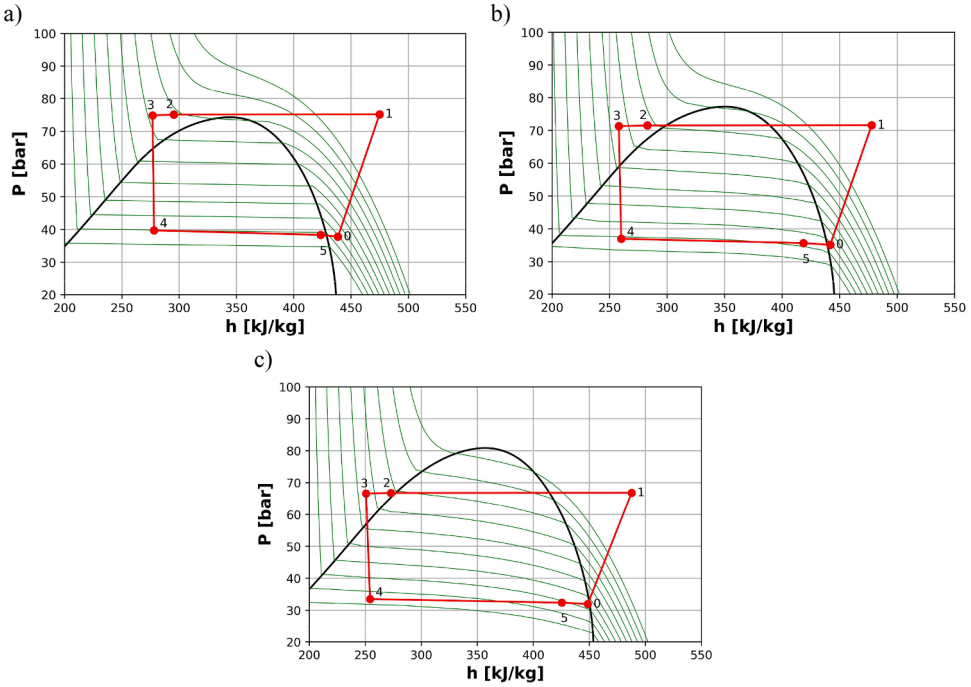

Fig. 6. Ph diagram for $T_{w0} = 30$°C; a) pure CO_2, b) mixture with 5 % DME c) mixture with 10 % DME.

between point 5–0 and 2–3. This may be due to the fact that the IHX in this case does not contain significant quantities of liquid.

When a 5 % of DME is added, the cycle changes significantly (Fig. 6b). The COP rises to 4.04. The condensation pressure lowers to 71.5 bar. Another fundamental difference is evident from the graph: point 5 (end of evaporation) is now well within the two-phase region. This circumstance stems from the optimization of the temperature glide at the evaporator, i.e. this position of point 5 gives a good match between the temperature rise of the water/glycol mixture (5 °C) and the variable evaporation temperature of the CO_2/DME mixture. Furthermore, the residual latent heat available between points 5 and 0 improves the heat transfer within the IHX and hence contributes to the performance improvement.

When a 10 % of DME is added, the results change as shown in Fig. 6c. As already seen in Fig. 2, the increase of DME percentage does not give an improvement in terms of COP. In the case of the cycle depicted in Fig. 6c, the COP is 3.96, i.e. very close, but slightly lower than that obtained with 5 %.

The marginal decrease in COP could be attributed to the increased proportion of DME, which expands the cycle and shifts points 3 and 4 to the left. While this enhances the cooling capacity, it also widens the temperature glide to 6.9 °C, surpassing the temperature differential of the water-glycol mixture. Consequently, this elevates the heat-transfer irreversibility at the evaporator. The reduction in condensation pressure to 66.8 bar is insufficient to compensate this issue.

3.2.2. Case $T_{w0} = 35°C$

For the case T_{w0} =35 °C, pure CO_2 produces the cycle shown in Fig. 7a. The cycle is clearly transcritical and rather "narrow", i.e. vapour quality at evaporator inlet is high. Consequently, the IHX has a limited effectiveness because it is empty of liquid. Correspondingly, the COP is as low as 2.74. The gas cooler pressure must now be optimized, and in this case it is as high as 84.9 bar. When a 5 % of DME is added, the critical temperature of the mixture increases to 36.1 °C and hence the cycle becomes wider and passes very close to the critical point, as shown in Fig. 7b. The COP increases to 2.88, while the temperature glide is 2.2 °C. Finally, a mixture with 10 % DME has a critical temperature of 39.9 °C, so that the cycle becomes clearly subcritical and widens even more, as shown in Fig. 7c. The COP raises to 3.15.

3.2.3. Case $T_{w0} = 40°C$

The cycle pure CO_2 at T_{w0} = 40 °C shown in Fig. 8a is not dissimilar from the one shown in Fig. 8a, but the optimum gas cooler pressure raises to 94 bar with a COP of 2.05. Adding a 5 % of DME produces the modifications shown in Fig. 8b. The COP is raised to 2.15. Finally, adding a 10 % of DME gives a cycle as shown in Fig. 8c. The COP is further raised to 3.09. The temperature glide is exactly 5 °C, giving a perfect match with the water-glycol mixture.

3.3. Parametric study

Fig. 9a shows the electric power consumed by the compressor as a function of maximum cycle pressure P_1. A definite, practically linear trend is evident. More precisely, the lower line groups together the points referring to pure CO_2 and 5 % DME at 35 and 40 °C, while the points referring to 10 % DME and 5 % DME at 30 °C are slightly higher. In any case, the vertical distance between the points is so small that, when a reduction of P_1 of the order of 10 bars is considered, the addition of DME surely reduces the power consumption.

The system cooling capacity is shown in Fig. 9b. As can be seen, the 9 curves are grouped as the COP curves in Fig. 2, but the cooling capacity always increases with the gas cooler (or condenser) pressure. The combination of this trend with the one of the power consumed by the compressor gives rise to the maximum COP points shown in Fig. 2. Pure CO_2 exhibits a cooling capacity comparable to that of the mixtures. Only in the case of $T_{w0} = 40$ °C does the CO_2 cooling capacity consistently surpass that of the mixtures. However, when comparing the maximum COP points, the disparities are not so pronounced: the cooling powers are 1892, 1833, and 1774 W, respectively, for pure CO_2, 5 % DME, and 10 % DME. In other words, only a 6 % is lost in terms of cooling power. Apparently, the loss in volumetric heating capacity is compensated by the improved efficiency, and hence the system may basically satisfy the same cooling load with lower energy consumption.

Fig. 10a shows that for a given pressure P_1, the compression ratio increases as the DME percentage increases. However, Fig. 9a shows that

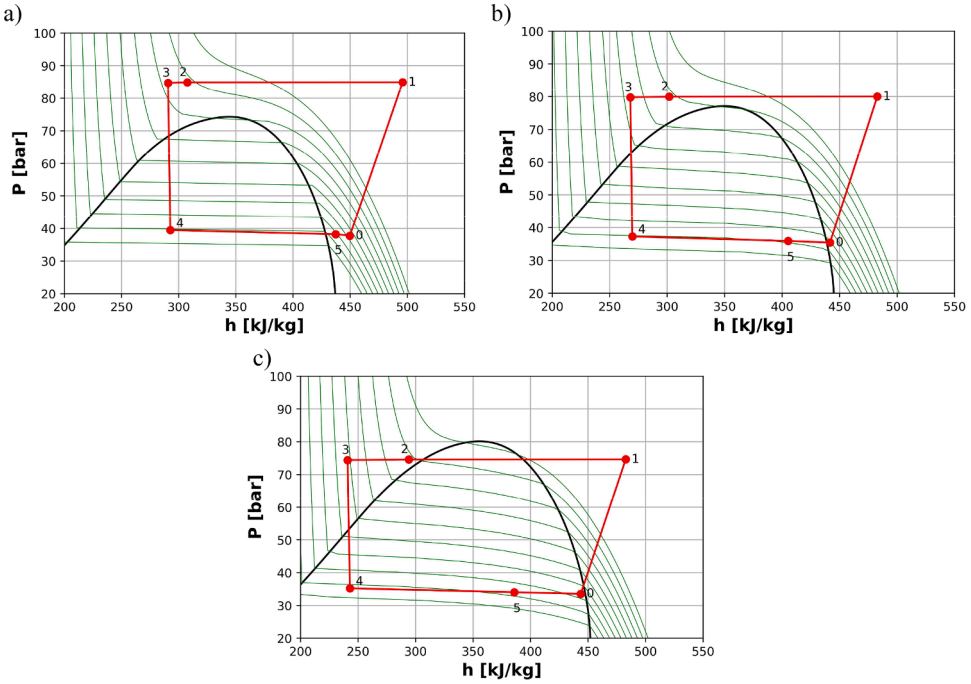

Fig. 7. Ph diagram for T_{w0} = 35°C: a) pure CO_2, b) 5 % DME, c) 10 % DME.

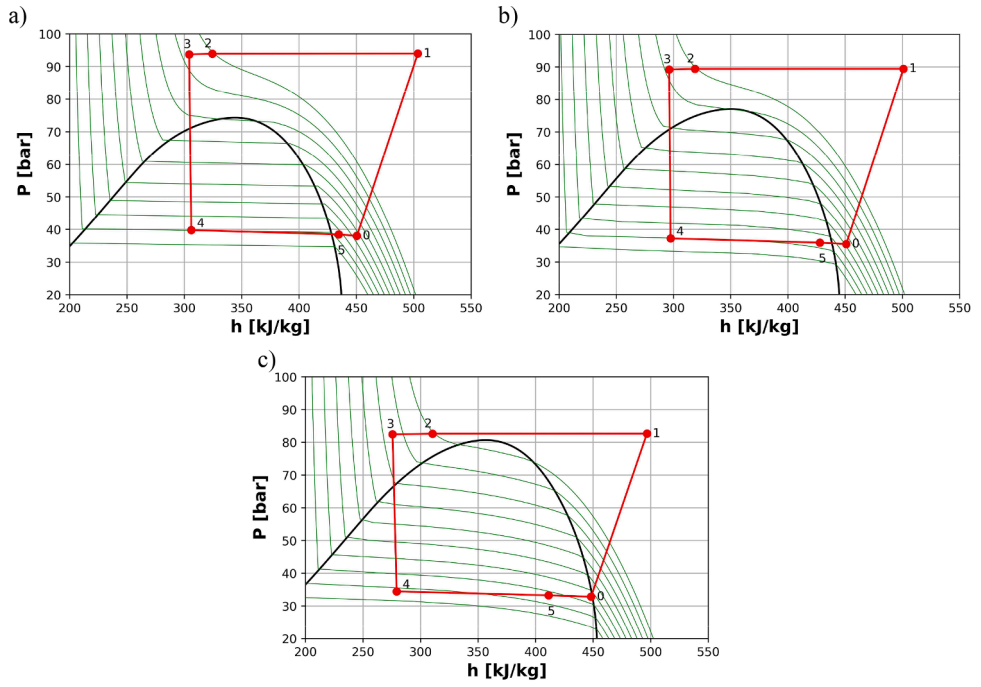

Fig. 8. Ph diagram for $T_{w0} = 40$°C: a) pure CO_2, b) 5 % DME, c) 10 % DME.

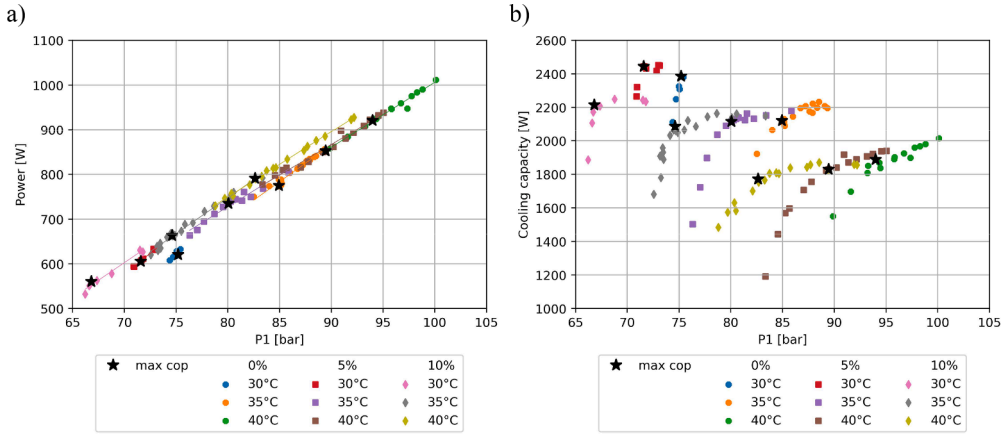

Fig. 9. Compressor: a) Electric power consumed, b) Cooling capacity.

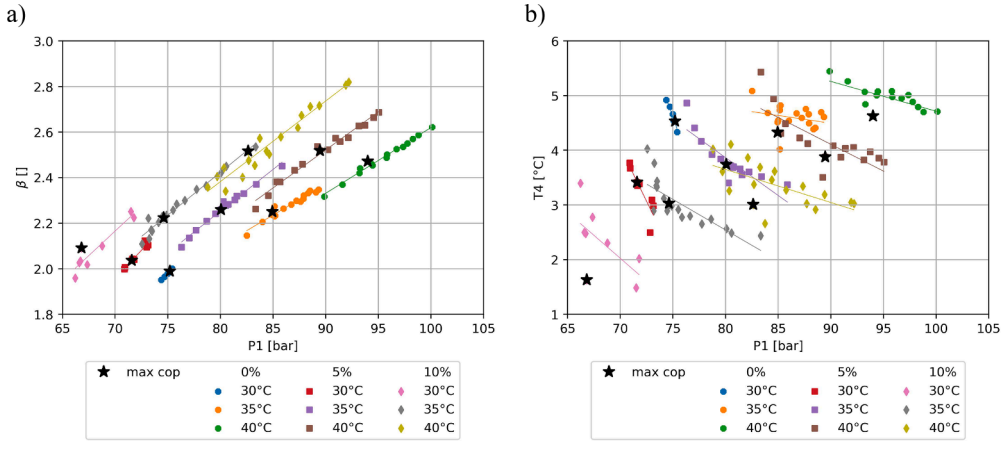

Fig. 10. a) Compression ratio, b) Evaporator inlet temperature.

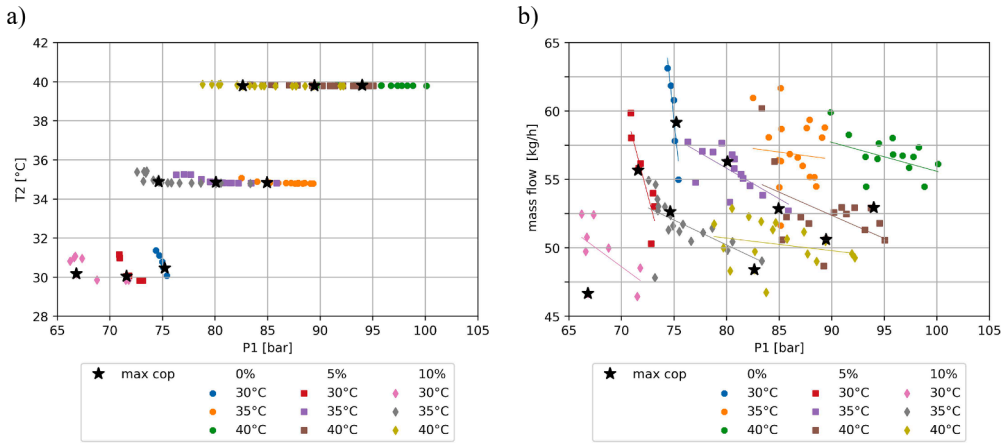

Fig. 11. a) Condenser/gas cooler exit temperature, b) Mass flow rate.

actually input work does not increase that much. This is due to the mass flow rate decrease, which is due to the reduced compressor inlet pressure. The black stars show the optimum conditions in terms of COP and quite evidently are located at roughly the same compression ratio for a given water inlet temperature. An exception is registered in the case marked as 30 °C, as will be explained later.

Another evidence in Fig. 10a is that curves at constant composition and P_1, (e.g. yellow, grey or pink curves) have a higher compression ratio as temperature T_{w0} decreases. This may be explained from Fig. 10b, where the evaporator inlet temperature T_4 is seen to decrease as T_{w0} decreases. The reason of this behaviour is related to the heat exchange at the evaporator. The enthalpy difference available at the evaporator increases, causing an increased temperature glide and hence an increased pinch point temperature difference between the evaporating fluid and the water/glycol. Henceforth the compressor inlet pressure decreases, increasing β.

Fig. 11a shows the condenser/gas cooler exit temperature (T_2) as a function of pressure P_1. The dots on top of the figure are all aligned and very close to the water inlet temperature $T_{w0} = 40\ ^{\circ}C$. The intermediate series refers to $T_{w0} = 35\ ^{\circ}C$. The temperature of the working fluid shows some variations at low P_1.

The variations for $T_{w0} = 30\ ^{\circ}C$ are much more evident. This variability is due to the fact that the gas-cooler/condenser works differently in these cases. For the case at 40 °C, the cycle is transcritical and the coupling between the working fluid temperature and the water temperature is better. Therefore the dots are all aligned and very close to the water temperature (the gas cooler has a huge heat exchange surface). In the case of the dots in the middle of the figure (which correspond to $T_{wo} = 35\ ^{\circ}C$), when the pressure decreases, the temperature T_2 increases slightly. In the case of the dots on the lower left corner, the situation is more complex. An explanation can be proposed referring to the blue dots (pure CO_2). If we open the throttle valve and the high-pressure P_1 decreases, the superheat is reduced and the density at the inlet of the compressor is increased. Hence, the increased mass flow rate (Fig. 11b) produces a worse heat exchange at the gas cooler, the water mass flow rate being constant. Fig. 11b shows that increasing the DME concentration, the mass flow rate decreases, as expected due to the lower density.

Fig. 12 illustrates the vapor quality at the evaporator inlet. Within each group of experimental points (same shape and color), we

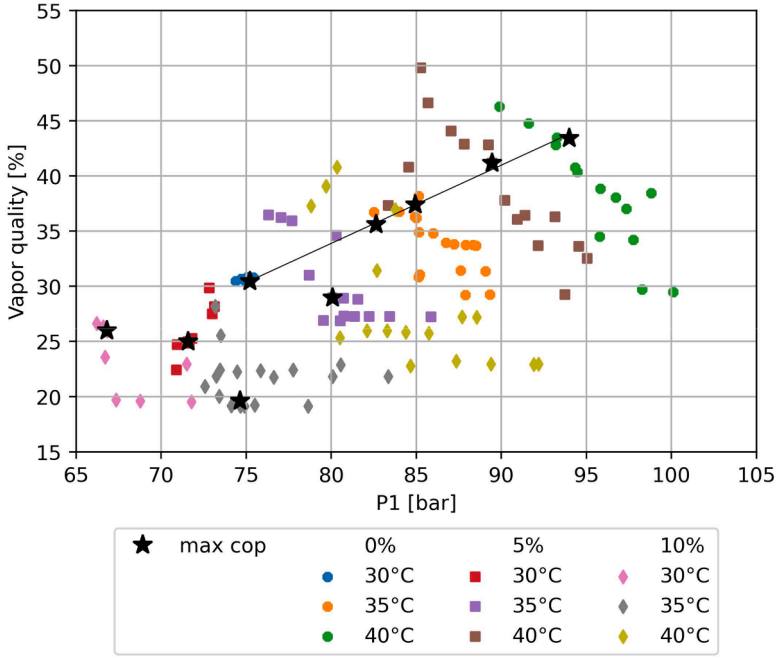

Fig. 12. Vapor quality.

Table 2
Experimental data.

	0 %	0 %	0 %	5 %	5 %	5 %	10 %	10 %	10 %
T_0 [C]	8.4	15.2	16.1	8.1	8.1	14.2	10.7	10.6	11.3
T_1 [C]	65.9	85.9	96.4	66.2	75.2	92.5	70.1	72.5	86.8
T_4 [C]	4.5	4.3	4.6	3.4	3.7	3.9	1.6	3.0	3.0
T_5 [C]	4.1	6.7	5.8	6.2	5.9	7.0	8.5	6.6	8.0
T_{w0} [C]	29.8	34.8	39.8	29.8	34.8	39.8	29.9	34.8	39.8
T_{w1} [C]	34.0	38.7	43.5	34.1	38.8	43.3	33.7	38.6	43.2
T_{wg0} [C]	12.4	12.1	12.1	12.6	12.0	11.9	12.1	12.0	12.0
T_{wg1} [C]	7.0	7.0	7.0	7.0	7.0	7.0	7.0	7.0	7.0
T_2 [C]	30.5	34.8	39.8	30.0	34.8	39.8	30.2	34.9	39.8
T_3 [C]	27.5	32.3	36.8	24.4	28.2	36.3	24.5	21.4	33.3
m_{liq} [kg/h]	41.2	33.1	29.9	41.8	40.0	29.8	34.5	42.3	31.2
m_{vap} [kg/h]	18.0	19.8	23.0	13.9	16.3	20.8	12.1	10.3	17.2
$\dot{V}_w$ [l/min]	10.1	10.1	10.1	10.1	10.1	10.1	10.1	10.1	10.1
$\dot{V}_{wg}$ [l/min]	6.9	6.6	5.8	6.9	6.7	5.9	6.8	6.6	5.6
P_4 [bar]	39.0	38.8	39.1	36.3	36.6	36.5	32.9	34.6	33.8
P_5 [bar]	38.4	38.2	38.5	35.7	35.9	35.9	32.4	34.0	33.3
P_0 [bar]	37.8	37.7	38.0	35.1	35.4	35.5	32.0	33.6	32.8
P_1 [bar]	75.2	84.9	94.0	71.6	80.1	89.5	66.8	74.6	82.6
P_2 [bar]	75.1	84.9	93.9	71.5	80.0	89.4	66.8	74.6	82.6
P_3 [bar]	74.9	84.8	93.7	71.3	79.8	89.2	66.6	74.4	82.4
W [W]	620.2	774.7	920.9	605.2	734.3	852.4	560.1	663.2	790.6
COP [-]	3.85	2.74	2.05	4.05	2.88	2.15	3.96	3.15	2.24
ΔCOP [%]	0	0	0	+5.2 %	+5.1 %	+4.9 %	+2.9 %	+15.0 %	+9.3 %
Q_{ref} [W]	2389.9	2124.3	1891.5	2448.5	2118.6	1832.6	2218.2	2090.1	1774.4
ΔQ_{ref} [%]	0	0	0	+2.5 %	−0.3 %	−3.1 %	−7.2 %	−1.6 %	−6.2 %

experimented different qualities for each P_1. By using the two valves positioned after the separator, we can control the superheat at the IHX exit. By reducing superheat, the IHX efficiency is increased, because the liquid volume inside it increases. For a given P_1, enhancing IHX efficiency leads to a decrease in vapor quality at the evaporator inlet.

For pure CO_2, the optimal condition occurs when the evaporator exit is superheated. Hence the Internal Heat Exchanger (IHX) has a low efficiency, and the quality at the evaporator inlet tends to be high. The graph shows that for a subcritical condition (light blue dots) the quality at the evaporator inlet is constant, while for transcritical cycles (orange and green dots) the quality decreases as P_1 increases.

For mixtures, the data is more varied because we experimented with different superheat levels at the IHX exit for the same P_1. Interestingly, connecting the optimal points (black stars) of each group reveals a linear trend for both pure CO_2 and mixtures at 40 °C.

However, the results for mixtures at 35 °C (purple and grey symbols) exhibit a different trend. As T_{w0} decreases, the enthalpy difference at the evaporator increases. Therefore, in order to match the water-glycol temperature difference, the quality at evaporator inlet that gives the best COP is reduced.

Finally, for the mixtures at 30 °C (pink and red groups), the optimal vapor quality stops decreasing, because it must be high enough to avoid a two-phase fluid at compressor inlet. Figs. 6b and 6c have already shown that, in both cases, the fluid at compressor inlet is saturated vapor.

Table 2 summarizes all the experimental data obtained for the nine cases discussed in the preceding analysis. Additional points were obtained during the experimental campaign; however, for the sake of brevity, they were not included in this study, but are available as supplementary material.

4. Conclusion

The experimental findings outlined in this paper validate the potential of the CO_2/DME mixture as a viable working fluid for cooling systems. In reference to air conditioning applications, calculations reported in Vaccaro et al. (2024) assert a 25 % enhancement in COP compared to pure CO_2. However, the experimental results demonstrate a maximum COP increase of 15 % (for a mixture containing 10 % DME, with a condensation temperature of 35 °C).

The discrepancy of the experimental result with respect to the calculations may be explained taking in account the differences in boundary conditions, the simplifying assumption used in the modelling and the measurement error on the composition of the mixture used in the experiments. Combining experimental data with thermodynamic analysis, our work suggests that the real DME percentage in the circuit was lower than the one introduced during the charge. This may be due to the preferential absorption of DME in the lubricant and to the different composition of the liquid and vapour phase in the separators. If the gaseous refrigerant is considered, considering that the DME concentration in the gaseous phase is lower than in the liquid phase, more DME can be used and an increased performance may be obtained, without surpassing the flammability level.

Furtheremore, the performance of the IHX is not always optimal. For instance, the scenario involving 10 % DME at 30 °C is penalized by a glide of 6.9 °C, exceeding the 5 °C temperature drop of the water-glycol. If the performance of the IHX could be improved, this glide would be reduced, resulting in a higher cycle COPs.

In any case, the result seems interesting and deserves further analysis. It is worth to recall that this mixture is non-flammable, non-toxic and has a GWP of 1. Furthermore, the advantages of CO_2 in terms of high volumetric cooling power, low pressure losses and high heat transfer coefficient, given the low quantity of DME added, change by a small amount.

Declaration of competing interests

The authors declare that they have no known competing financial interests or personal relationships that could have appeared to influence the work reported in this paper.

Acknowledgment

Supported by PNRR - Missione 4 “Istruzione e Ricerca” - Componente C2 Investimento 1.1 “Fondo per il Programma Nazionale di Ricerca e Progetti di Rilevante Interesse Nazionale (PRIN)”, “Next generation inverse cycles using CO2 based mixtures as refrigerant (CO2MIX)”, project code: P2022C494T, MUR D.D. financing decree n. 1385 of 01/09/2023 (CUP B53D23026960001) funded by the European Commission under the NextGeneration EU programme"

Supplementary materials

Supplementary material associated with this article can be found, in the online version, at doi:10.1016/j.ijrefrig.2024.10.002.

References

Afroz, H.M., Miyara, A., Tsubaki, K., 2008. Heat transfer coefficients and pressure drops during in-tube condensation of CO2/DME mixture refrigerant. Int. J. Refrig. 31 (8), 1458–1466.

Bouteiller, P., Tobaly, P., Terrier, M.F., Toublanc, C., 2015. Experimental Bench Design for Heat Pump Using CO_2 Based Mixtures. In: 24th IIR International Congress of Refrigeration pp. paper-n.

Bouteiller, P., Terrier, M.F., Tobaly, P., 2017. Experimental study of heat pump thermodynamic cycles using CO2 based mixtures-Methodology and first results. In: AIP Conference Proceedings, 1814. AIP Publishing.

Bouteiller, P., 2017. *Etude expérimentale de cycles de pompe à chaleur utilisant des mélanges à base de CO2* (Doctoral dissertation. Conservatoire National Des Arts Et metiers-CNAM).

Caramaschi, M., Ommen, T.S., Kærn, M.R., Østergaard, K., Poppi, S., Madani, H., Elmegaard, B., 2022. Modelling natural refrigerant mixtures for residential heat pump applications in Python. In: 15th IIR-Gustav Lorentzen Conference on Natural Refrigerants. International Institute of Refrigeration, p. 0153.

Caramaschi, M., Notturno, J., Vaccaro, G., Meesenburg, W., Jensen, J., Elmegaard, B., Tobaly, P., 2024. Propylene and DME solubility in PAG oil: Experimental investigations and simplified modeling. Int. J. Refrig.

Di Nicola, G., Polonara, F., Stryjek, R., Arteconi, A., 2011. Performance of cascade cycles working with blends of CO2+ natural refrigerants. Int. J. Refrig. 34 (6), 1436–1445.

Johansson, A., Lundqvist, P., 2001. A method to estimate the circulated composition in refrigeration and heat pump systems using zeotropic refrigerant mixtures. Int. J. Refrig. 24 (8), 798–808.

Koyama, S., Jin, D.X., Xue, J., Takata, N., Kuwahara, K., Miyara, A., 2007. Experimental Study on the Performance of a CO2/DME System. In: Proceedings, pp. 1678–1684.

Lemmon, E.W., B, I.H., L, H.M., O, M.M., 2018. NIST Standard Reference Database 23: Reference Fluid Thermodynamic and Transport Properties-REFPROP. Version 10.0. National institute of standards and technology, Gaithersburg, Maryland. M. https://doi.org/10.18434/T4/1502528.

Martínez-Ángeles, M., Nebot-Andres, L., Calleja-Anta, D., Llopis, R., 2024. Experimental assessment of CO2/R-152a mixtures in a refrigeration plant with integrated mechanical subcooling. Int. J. Refrig. 158, 288–302.

Massuchetto, L.H.P., do Nascimento, R.B.C., de Carvalho, S.M.R., de Araújo, H.V., d'Angelo, J.V.H., 2019. Thermodynamic performance evaluation of a cascade refrigeration system with mixed refrigerants: R744/R1270, R744/R717 and R744/RE170. Int. J. Refrig. 106, 201–212.

Onaka, Y., Miyara, A., Tsubaki, K., & Koyama, S. (2008). Analysis of heat pump cycle using CO2/DME mixture refrigerant.

Onaka, Y., Miyara, A., Tsubaki, K., 2010. Experimental study on evaporation heat transfer of CO2/DME mixture refrigerant in a horizontal smooth tube. Int. J. Refrig. 33 (7), 1277–1291.

Sánchez, D., Larrondo, R., Vidan-Falomir, F., Cabello, R., 2024. Experimental evaluation of the CO2-based mixtures CO2/R32, CO2/R1234yf and CO2/R1270 in a transcritical refrigerating plant considering the effect of the internal heat exchanger (IHX). Appl. Therm. Eng. 236, 121473.

Sánchez, D., Vidan-Falomir, F., Nebot-Andrés, L., Llopis, R., Cabello, R., 2023. Alternative blends of CO2 for transcritical refrigeration systems. Experimental approach and energy analysis. Energy Convers. Manage 279, 116690.

Sicco, E., Martínez-Ángeles, M., Toffoletti, G., Nebot-Andrés, L., Sánchez, D., Cabello, R., Llopis, R., 2024. Experimental evaluation of CO2/R-152a mixtures in a refrigeration plant with and without IHX. Int. J. Refrig.

Tobaly, P., Terrier, M.F., Bouteiller, P., 2018. CO_2+ propane mixture as working fluid for refrigeration in hot climates. Experimental results of energy efficiency tests. In: 13th IIR Gustav Lorentzen conference on natural refrigerants: natural refrigerant solutions for warm climate, pp. 18–20.

Tsang, C.Y., Streett, W.B., 1981. Vapor-liquid equilibrium in the system carbon dioxide/dimethyl ether. J. Chem. Eng. Data 26 (2), 155–159.

Vaccaro, G., Milazzo, A., Talluri, L., 2023. Thermodynamic assessment of trans-critical refrigeration systems utilizing CO_2-based mixtures. Int. J. Refrig. 147, 61–70.

Vaccaro, G., Milazzo, A., Talluri, L., 2024. A proposal for a non-flammable, fluorine-free, CO_2-based mixture as a low TEWI refrigerant. Int. J. Refrig. 158, 157–163.

Youbi-Idrissi, M., 2003. *Impact de l'huile de lubrification sur les performances thermodynamiques des pompes à chaleur réversibles* (Doctoral dissertation. Conservatoire National Des Arts Et metiers-CNAM).

Yu, B., Wang, D., Liu, C., Jiang, F., Shi, J., Chen, J., 2018. Performance improvements evaluation of an automobile air conditioning system using CO2-propane mixture as a refrigerant. Int. J. Refrig. 88, 172–181.

Yu, B., Yang, J., Wang, D., Shi, J., Guo, Z., Chen, J., 2019. Experimental energetic analysis of CO2/R41 blends in automobile air-conditioning and heat pump systems. Appl. Energy 239, 1142–1153.